05

Cyclic stability of superelasticity and elastocaloric effect in $Ni_{54}Fe_{19}Ga_{27}$ single crystals

© E.I. Yanushonite, E.Yu. Panchenko, A.B. Tokhmetova, Yu.I. Chumlyakov

Tomsk State University, Tomsk, Russia
E-mail: yanushonite98@mail.ru

Received November 6, 2024
Revised December 17, 2024
Accepted December 20, 2024

The cyclic stability of superelasticity and elastocaloric effect under compression deformation in initial and aged at 773 K, 1 h [001]-single crystals of $Ni_{54}Fe_{19}Ga_{27}$ alloy (at.%) was investigated. It was established that single crystals exhibit high cyclic stability of the elastocaloric effect with a stable value of $\Delta T_{ad} = 9.2 \pm 0.5$ K (for initial) and 8.2 ± 0.5 K (for aged) up to 10^5 load/unload cycles without sample destruction. The conditions of high stability and microstructural mechanisms of degradation of superelasticity parameters in single crystals of $Ni_{54}Fe_{19}Ga_{27}$ alloy are analyzed.

Keywords: single crystal, superelasticity, elastocaloric effect.

DOI: 10.61011/TPL.2025.04.61009.20178

Recently, there has been a significant amount of interest in the study of the elastocaloric effect (ECE) in shape memory alloys for the development of environmentally friendly solid-state cooling devices and heat pumps. The cooling capacity of a material manifesting the ECE is determined by isothermal change in entropy ΔS and/or adiabatic change in temperature ΔT_{ad} in the course of a thermoelastic martensitic transformation (MT) under load within the temperature range of superelasticity (SE) [1–3]. A large ECE magnitude (ΔT_{ad} up to 30 K) in the working cycle is observed in shape memory alloys based on NiTi, CuAlMn, and NiMnTi [3–6]. In addition to a high ΔT_{ad} value, a high cyclic ECE stability, low deforming stresses, and narrow mechanical hysteresis $\Delta\sigma$, which affects primarily the coefficient of performance (COP_{mat}) of a material and the cyclic ECE stability, deserve a mention among the parameters important for practical applications. In contrast to NiTi alloys, NiFeGa alloys, which undergo the $B2(L2_1)$–$10M/14M$–$L1_0$ MT, have 2–4 times lower deforming stresses, a narrow $\Delta\sigma = 15-30$ MPa, and a high cyclic stability of SE parameters [3,4,7,8]. Therefore, these NiFeGa alloys are regarded as promising elastocaloric materials. It has been demonstrated earlier that aged NiFeGa polycrystals containing γ-phase particles maintain a stable ECE value up to 3.2 K over 200 loading/unloading cycles. However, when the number of cycles increases to 500, ΔT_{ad} decreases by 19% [3]. Compared to polycrystals, [001] NiFeGa single crystals aged at 773 K for 1 h ($\Delta T_{ad} = 9.0$ K) and at 1373 K for 0.5 h ($\Delta T_{ad} = 8.5$ K) have higher ECE values stable over 150 cycles [7]. The cyclic stability of ΔT_{ad} in NiFeGa single crystals is facilitated by the chosen [001] orientation. Single crystals of NiFeGa alloys oriented along the [001] direction are, first, high-strength materials when deformed by compression; the dislocation yield strength of austenite and martensite exceeds 800 and 1500 MPa, respectively [8,9]. Second, martensite detwinning does not contribute to the transformation deformation in the course of martensitic transformations under load in [001] crystals. With such orientations, a narrow $\Delta\sigma$, which depends only weakly on temperature and applied stresses, is observed during the MT under load, and the cyclic SE stability is high [7,8]. A high cyclic stability of SE and ECE with $\Delta T_{ad} = 9.8$ K was demonstrated in [5] for single-phase [001] $Ni_{54}Fe_{19}Ga_{27}$ single crystals over 10^4 loading/unloading cycles. However, literature data on the influence of $\gamma(\gamma')$-phase particles on the cyclic stability of the SE and ECE parameters are currently lacking, and the relation between the microstructure variation and the SE and ECE parameters in long-term cyclic tests of [001] NiFeGa single crystals has not been established. Therefore, the aim of the present study is to examine the influence of cyclic loading/unloading on the microstructure and the SE and ECE parameters of the as-grown [001] $Ni_{54}Fe_{19}Ga_{27}$ single crystals and the crystals aged at 773 K for 1 h.

The studied single crystals of the $Ni_{54}Fe_{19}Ga_{27}$ alloy were grown by the Bridgman method. The experimental procedure was detailed in [7]. The cyclic SE and ECE stability was examined in up to 10^5 cycles at room temperature using an Electro Puls E3000 electrodynamic testing system at a loading rate of $1.67 \cdot 10^{-2}\,s^{-1}$ and unloading rate of $6.7 \cdot 10^{-1}\,s^{-1}$ to establish such conditions that are as close as possible to the adiabatic ones. The ΔT_{ad} value for ECE was measured by contact using a T-type thermocouple with thermal paste applied between the thermocouple and the sample surface. The ECE measurement error was ± 0.5 K.

The microstructure of crystals before and after aging in austenite at 773 K for 1 h was studied using a Hitachi HT-7700 transmission electron microscope (TEM) provided by the Krasnoyarsk Regional Research Equipment Sharing Center of the Federal Research Center „Krasnoyarsk Sci-

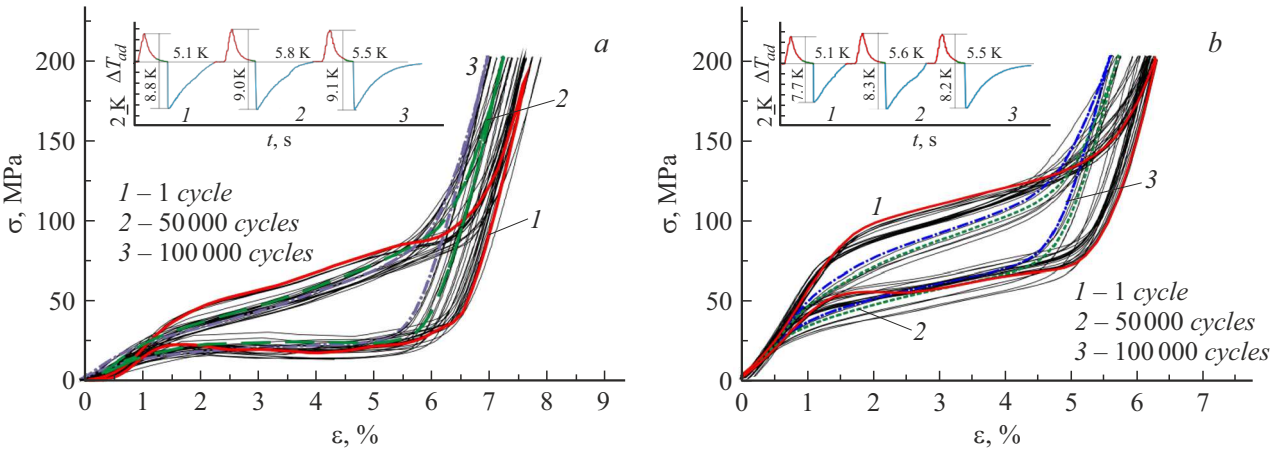

Figure 1. Curves $\sigma(\varepsilon)$ obtained in the study of the cyclic SE and ECE stability in [001] $Ni_{54}Fe_{19}Ga_{27}$ single crystals. *a* — As-grown single crystals; *b* — single crystals aged at 773 K for 1 h. A color version of the figure is provided in the online version of the paper.

Characteristic temperatures of the MT, thermal characteristics, and the maximum theoretical ΔT_{ad}^{t} and experimental $\Delta T_{ad}^{exp}(\max)$ ECE values for [001] $Ni_{54}Fe_{19}Ga_{27}$ single crystals

State	M_s, K (±2)	M_f, K (±2)	A_s, K (±2)	A_f, K (±2)	C_p, J/(kg · K)	α_{Ms}, MPa/K	ΔS^{A-M}, J/(kg · K)	ΔT_{ad}^{t}, K	ΔT_{ad}^{exp} (max), K (±5)
As-grown [8]	276	265	280	289	488	2.5	−18.6	10.8	10.9
Aged at 773 K, 1 h [7]	259	245	257	270	434	2.7	−17.2	10.5	11.1

ence Center of the Siberian Branch of the Russian Academy of Sciences." The obtained results were discussed in detail in our studies [7,8]. It was found that the as-grown single crystals synthesized at room temperature are in the $L2_1$-austenite phase and contain a small volume fraction (less than 2 %) of incoherent γ'-phase particles 2–5 μm in size with an ordered $L1_2$ crystal structure. Aging leads to additional precipitation of γ'-phase particles with sizes ranging from 170 to 500 nm; i.e., a bimodal distribution of particle sizes is observed in aged single crystals.

The MT temperatures and specific heat capacity C_p of single crystals were determined by differential scanning calorimetry (see the table). Following aging, the MT temperatures decrease by 17 K compared to the values for the as-grown crystals due to a change in the chemical composition of the matrix in the process of precipitation of particles, the effects of dispersion strengthening, and the growth of elastic and surface energies that are needed to maintain the conformity of the martensitic matrix deformation and the elastic deformation of nanosized particles of the γ'-phase. It was demonstrated in [7,8] that the magnitude of ECE during the MT under load may be estimated using the coefficient of temperature increase of critical stresses $\alpha_{Ms} = d\sigma_{Ms}/dT$ for determination of the magnitude of entropy change ΔS^{A-M} in the course of transformation. The following relation may be used to estimate the maximum value of adiabatic cooling ΔT_{ad}^{t} in the case of ECE [5,8]:

$$\Delta T_{ad}^{t} = \frac{T_0 \Delta S}{C_p} = \frac{1}{\rho C_p}\frac{d\sigma_{Ms}}{dT}\varepsilon_0 T_0, \qquad (1)$$

where T_0 is the equilibrium temperature between austenite and martensite phases and ε_0 is the transformation deformation. It follows from the table that the precipitation of particles during aging in austenite leads to a 8 and 11% reduction (compared to the as-grown single crystals) in both the magnitude of entropy change ΔS^{A-M} and specific heat capacity C_p of the material, respectively. Since ΔT_{ad}^{t} is directly proportional to ΔS^{A-M} and inversely proportional to C_p, ΔT_{ad}^{t} does not decrease in any significant way in aged crystals containing non-transformed particles. As the calculations show, the ΔT_{ad}^{t} values for the as-grown and aged single crystals are close and agree well with the maximum experimental ΔT_{ad} values for these crystals (see the table).

In the present study, the cyclic stability of SE and ECE was investigated at room temperature under such conditions when the specified stress level remained constant at 200 MPa. The SE and ECE curves for the studied crystals corresponding to 1–10^5 cycles are shown in Fig. 1. The dependences of critical stresses σ_{Ms}, mechanical $\Delta\sigma$, and ΔT_{ad} on the number of loading/unloading cycles are presented in Fig. 2. It has been demonstrated for the first time that $Ni_{54}Fe_{19}Ga_{27}$ single crystals feature a high ECE stability

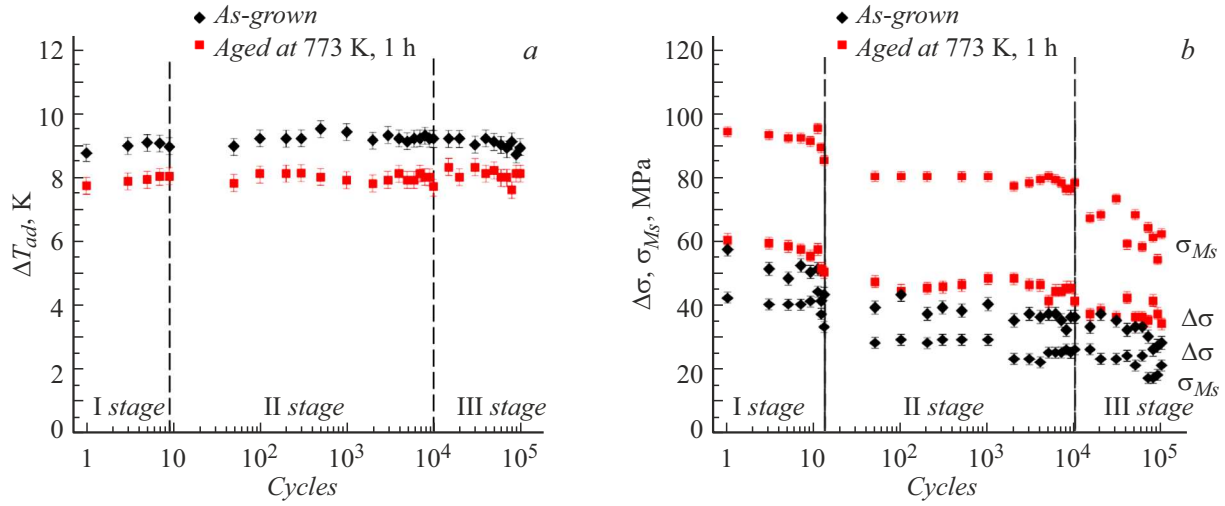

Figure 2. Dependences of the SE parameters on the number of cycles for the as-grown [001] $Ni_{54}Fe_{19}Ga_{27}$ single crystals and crystals aged at 773 K for 1 h. *a* — Dependence of ΔT_{ad} on the number of cycles; *b* — dependences of $\Delta\sigma$ and σ_{Ms} on the number of cycles.

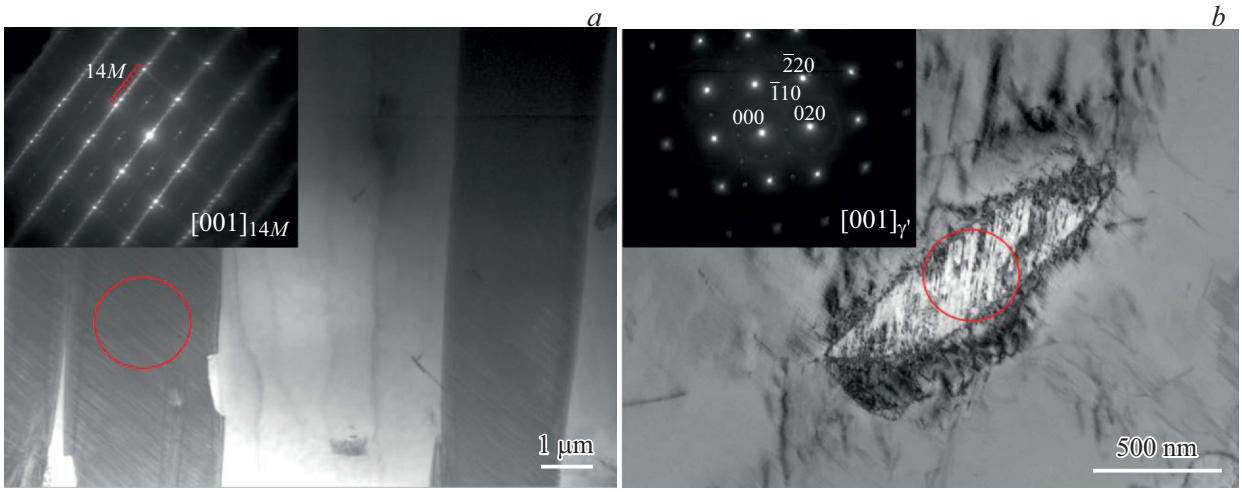

Figure 3. Microstructure of the as-grown [001] $Ni_{54}Fe_{19}Ga_{27}$ single crystals and crystals aged at 773 K for 1 h imaged after 10^5 cycles with a TEM. *a* — As-grown single crystals: bright-field image of the matrix and residual 14*M* martensite with the corresponding microdiffraction pattern, zone axis $[001]_{14M}$; *b* — aged single crystals: bright-field image of the matrix and a particle of the γ'-phase with the corresponding microdiffraction pattern from the particle, zone axis $[001]_{\gamma'}$.

over up to 10^5 cycles with the values of $\Delta T_{ad} = 9.2 \pm 0.5$ K (for the as-grown crystals) and 8.2 ± 0.5 K (for the aged ones), which are close to the maximum ECE values (see the table). No degradation of ΔT_{ad} was detected during cyclic testing; the sample after 10^5 cycles had no cracks and remained in working condition (Fig. 2, *a*). However, the SE parameters deteriorated. Three stages of deterioration of SE parameters may be distinguished during cyclic testing (Fig. 2, *b*). At stage I (from the first cycle to cycles 13–15), σ_{Ms} decreases by 21 % in the as-grown crystals, while σ_{Ms} in the aged crystals decreases just by 10 %. Mechanical stress $\Delta\sigma$ in the as-grown and aged crystals decreases at stage I by 25 and 17 %, respectively. The degradation at this stage is associated with the accumulation of dislocations and a small fraction of residual martensite, which facilitate the nucleation of martensite crystals in subsequent cycles and reduce energy dissipation due to dislocation strengthening. The values of σ_{Ms} and $\Delta\sigma$ decrease as a result. After 13–15 loading/unloading cycles, the SE parameters in as-grown and aged crystals become stabilized.

With further cycling, the crystals enter stage II (extending from cycle 15 to 10^4 cycles), where they demonstrate a high cyclic SE stability: the values of σ_{Ms} and $\Delta\sigma$ vary within the error limit (±2 MPa). Thus, the as-grown and aged [001] crystals feature a long period of cyclic stability of the SE and ΔT_{ad} parameters that extends to 10^4 cycles.

At stage III (from 10^4 cycles to 10^5 cycles), σ_{Ms} decreases slowly by 9 % in both crystals, while $\Delta\sigma$ in the as-grown and aged crystals decreases by 22 and 17 %, respectively (compared to the SE parameter values

at stage II). Despite the variation of SE parameters, no accumulation of irreversible deformation is observed in the loading/unloading cycles; therefore, the entire material volume undergoes the MT, which leads to a constant ΔT_{ad} value.

The COP_{mat} value, which is numerically equal to the ratio of useful thermal energy that a sample may absorb from the environment during ECE to the energy dissipation value characterizing work $\frac{1}{\rho}\oint \sigma d\varepsilon$ expended within the loading/unloading cycle [1], is used to classify the elastocaloric properties of a material:

$$\mathrm{COP}_{mat} = \frac{C_p \Delta T_{ad}}{1/\rho \oint \sigma d\varepsilon}, \qquad (2)$$

where ρ is density ($8450\,\mathrm{kg}\cdot\mathrm{m}^{-3}$). The COP_{mat} value in cycles 1 to 13–15 (stage I) increases due to a reduction in energy dissipation during the MT and a suppression of mechanical hysteresis in the as-grown and aged crystals by 62 and 67 %, respectively. At stages II and III, stable values of $\mathrm{COP}_{mat} = 21$ for the as-grown crystals and $\mathrm{COP}_{mat} = 20$ for the aged crystals are observed. The COP_{mat} values obtained in the present study are higher than those of such elastocaloric shape memory alloys as $Cu_{73}Mn_{12}Al_{15}$ (polycrystal, $\mathrm{COP}_{mat} = 13.3$) [3], $Ni_{50}Fe_{19}Ga_{27}Co_4$ (single crystal, $\mathrm{COP}_{mat} = 14$) [2], $Ni_{53.2}Fe_{19.4}Ga_{27.4}$ (polycrystal, $\mathrm{COP}_{mat} = 14.5$) [3], $Co_{50}Ni_{20}Ga_{30}$ (single crystal, $\mathrm{COP}_{mat} = 16.4$) [2], and $(Ni_{51.5}Mn_{33}In_{15.5})_{99.7}B_{0.3}$ (polycrystal, $\mathrm{COP}_{mat} = 18$) [2]. Thus, high COP_{mat} values and the high cyclic stability of ECE parameters indicate that NiFeGa single crystals and polycrystals with a sharp texture along the [001] direction hold much potential for practical application in the field of solid-state cooling.

The following factors contribute to the high cyclic stability of SE parameters and the ECE value and the high values of coefficient of performance COP_{mat} upon stabilization of the SE loop in $Ni_{54}Fe_{19}Ga_{27}$ crystals. First, high-strength [001] crystals were chosen. Compared to other orientations, they provide minimal energy dissipation and a narrow mechanical hysteresis $\Delta\sigma$ during the MT. This is facilitated by the high resistance of austenite and martensite to dislocation slip; the progression of MT $L2_1-L1_0$ through the intermediate $14M$ phase (Fig. 3, *a*), which is characterized by high coherence and mobility of the interphase boundary; and the lack of detwinning of $L1_0$ martensite crystals under load. Second, the high cyclic stability of SE and ECE parameters is facilitated by the presence of γ'-phase particles. In the aged single crystals, small particles of the γ'-phase (up to 300 nm in size) do not undergo plastic deformation during cyclic tests and accumulate elastic energy in the course of direct MT, which facilitates reverse transformation. In contrast, large particles of the γ'-phase ($d > 300$ nm) in the as-grown and aged single crystals undergo plastic deformation (Fig. 3, *b*) and produce a significant contribution to the relaxation of internal stresses during the MT. Combined with the high strength properties of austenite and martensite, this leads to suppression of plastic deformation and degradation processes in the matrix during the MT in the process of cyclic testing.

Funding

This study was supported financially by the Russian Science Foundation, grant № 20-19-00153.

Conflict of interest

The authors declare that they have no conflict of interest.

References

[1] H. Mevada, B. Liu, L. Gao, Y. Hwang, I. Takeuchi, Int. J. Refrig., **162**, 86 (2024). DOI: 10.1016/j.ijrefrig.2024.03.014
[2] M. Imran, X. Zhang, Mater. Des., **206**, 109784 (2021). DOI: 10.1016/j.matdes.2021.109784
[3] M. Imran, X. Zhang, M. Qian, L. Geng, Intermetallics, **136**, 107255 (2021). DOI: 10.1016/j.intermet.2021. 107255
[4] H. Chen, F. Xiao, X. Liang, Z. Li, X. Jin, N. Min, T. Fukuda, Scripta Mater., **162**, 230 (2019). DOI: 10.1016/j.scriptamat.2018.11.024
[5] Y. Wu, E. Ertekin, H. Sehitoglu, Acta Mater., **135**, 158 (2017). DOI: 10.1016/j.actamat.2017.06.012
[6] H. Wang, H.-Y. Huang, Y.-J. Su, J. Alloys Compd., **828**, 154265 (2020). DOI: 10.1016/j.jallcom.2020.154265
[7] E.Y. Panchenko, E.I. Yanushonite, A.S. Eftifeeva, A.B. Tokhmetova, I.D. Kurlevskaya, A.I. Tagiltsev, N.Y. Surikov, E.E. Timofeeva, Y.I. Chumlyakov, Metals, **12**, 1398 (2022). DOI: 10.3390/met12081398
[8] A. Eftifeeva, E. Panchenko, E. Yanushonite, I. Kurlevskaya, E. Timofeeva, A. Tokhmetova, N. Surikov, A. Tagiltsev, Y. Chumlyakov, Mater. Sci. Eng. A., **855**, 143855 (2022). DOI: 10.1016/j.msea.2022.143855
[9] F. Masdeu, J. Pons, J. Torrens-Serra, Y. Chumlyakov, E. Cesari, Mater. Sci. Eng. A., **833**, 142362 (2022). DOI: 10.1016/j.msea.2021.142362

Translated by D.Safin